Supporting Information

Sales-Carbonell et al. 10.1073/pnas.1217144110

SI Experimental Procedures

All animal procedures were conducted in accordance with standard ethical guidelines (European Communities Directive 86/60-EEC) and were approved by the local ethics committee (Comité d'Experimentació Animal, Universitat de Barcelona, Ref 520/08).

Animals. In vivo chronic electrocorticogram (ECoG) recordings were performed in three groups of animals: (*i*) 9 C57BL/6N (Charles River), (*ii*) conditional type 1 cannabinoid receptor (CB1R) mutant mice (4 Glu-CB1R$^{-/-}$, 5 GABA-CB1R$^{-/-}$, 4 CaMK-CB1R$^{-/-}$, and 7 D1-CB1R$^{-/-}$), and (*iii*) 13 WT littermates (1–3). All mice (male and female) were aged 4–7 mo. Regarding ECoG baseline activity and CP55940 effects on ECoG, no differences between sexes were observed. Similarly, no differences were observed between WT littermates of the four different mutant lines. Therefore, all WT animals were pooled into a single group for statistical comparison. Glu-CB1R$^{-/-}$ mice lack CB1R expression in dorsal telencephalon glutamatergic neurons, including neurons located in neocortex, paleocortex, archicortex, hippocampal formation, and cortical portions of the amygdala; GABA-CB1R$^{-/-}$ mice lack CB1R expression mainly from forebrain GABAergic neurons; CaMK-CB1R$^{-/-}$ mice lack CB1R expression in all forebrain principal neurons; and D1-CB1R$^{-/-}$ mice lack CB1R expression in cells expressing D1-type dopamine receptors, including striatal medium spiny neurons (1, 2, 4). Conditional CB1R mutant mice were generated in a predominant C57BL/6N background (back-crossed for at least five generations) and were genotyped before and after the experiments, as previously described (2). A few days before surgical implantations of chronic recording electrodes, animals were housed individually in the experimental laboratory in stable conditions of temperature (22 °C) and humidity (60%), with a constant cycle of 12 h light and 12 h dark and ad libitum access to food and water. Animals were given at least 1 wk of recovery time after the surgery before recordings started.

Surgical Procedures. All surgical procedures were performed with stereotaxic control under deep isoflurane anesthesia. In the majority of chronic recordings performed in mice, miniature stainless steel screws (Small Parts, size 000-120) were implanted epidurally above the somatosensory cortex [anteroposterior (AP): −0.5 mm; mediolateral (ML): ±3 mm, relative to Bregma). In a few mice, recordings were additionally performed above the prefrontal cortex (AP: +1.5; ML: ±0.75) and/or in the CA1 hippocampus pyramidal layer. Two miniatures screws implanted above cerebellum served as ground and reference.

For local injection experiments, mice were additionally implanted with a single stainless steel guide cannula (26 gauge; PlasticsOne) aimed at the dorsal border of the substantia nigra pars reticulata (AP: −3.4 mm; ML: ±1.37 mm; dorsoventral: −2.75 mm). The tip injector protruded 1 mm below the tip of the guide cannula.

Drugs Preparations. For i.p. injections, CP55940 and AM251 (Vitro) were dissolved in a 1:1:18 vehicle solution of DMSO (Sigma): cremophor-EL (Sigma):saline. The volume of the injections was 10 mL/kg of body weight. The dosage for CP55940 and AM251 i.p. injections was 0.3 and 3 mg/kg of body weight, respectively. For local injection experiments, 10 μg of CP55940, dissolved in 0.5 μL of vehicle (same as above), were injected. A muscimol (Tocris) solution (0.5 μL of 0.5 mg/mL in saline) and 0.5 μL of a (-)-bicuculline methiodide (Tocris) solution (0.2 mg/mL in saline) were also injected in WT and D1-CB1R$^{-/-}$ mice, respectively.

Chronic in Vivo Recordings and Local Injection Procedures. Wideband (0.1 Hz–8 kHz) neurophysiological signals (amplified 1,000 times via a Plexon HST/16V-G20 headstage and a Plexon PBX2 amplifier) and acceleration signals (1–50 Hz) were digitized at 1 kHz on two synchronized National Instruments A/D cards (PCI 6254, 16-bit resolution).

Locomotor activity was quantified either with two silver bipolar electromyography (EMG) electrodes inserted in the dorsal nuchal (neck) muscles or with a triple-axis miniature accelerometer affixed to the recording headstage (ADXL 335, SparkFun Electronics) (5). In this last case, the signal of the accelerometer *z* axis (vertical) was used.

Control recordings started 15 min after connection of the animal to the amplifier or vehicle i.p. injections. "Drug" recordings started 15 min after i.p. injections. Three types of experiments were performed: (*i*) vehicle-CP55940, (*ii*) vehicle-CP55940-AM251, and (*iii*) vehicle-AM251-[CP55940+AM251]. In the case of type-2 experiments, at least 2 h 30 min-long recordings were performed after AM251 injection to allow for complete reversion of the CP55940 effect. The ECoGs analyzed were then taken starting 1 h 30 min after AM251 i.p. injection. The rationale for this is the well-known slow reversibility of CB1R agonist effects by CB1R antagonist, which is explained by the lipophilic nature of CP55940 and AM251 and the better CB1R affinity of the former vs. the latter compound. One to three experiments were performed in each animal, depending on the quality of the electrophysiological signal. Experiments performed in the same animal were interleaved with at least 5 d without any injection.

For local injection procedures in awake mice, animals were manually restrained from the recording headstage, the dummy cannula was gently removed, and the injector was slowly inserted through the guide cannula. The injector was connected via a polyethylene tube (PE50; Plastics One) to a Hamilton microsyringe driven by a microinfusion pump (11 plus; Harvard Apparatus). A volume of 500 nL was injected at a rate of 200 nL/min. To allow complete diffusion of the drug, the injector was left in place 2 min after injection before being removed and replaced by the dummy. After baseline recording, the injection order was vehicle-CP55940-muscimol (or bicuculline in CB1R-D1$^{-/-}$ mice). Electrophysiological recordings consisted of at least 20 min of immobility epochs in each condition, starting just after local injections.

At the end of the experiments, mice were deeply anesthetized and their brain fixed with an intracardiac perfusion of 10% formalin solution. The brains were sliced (50 μm), and Nissl staining was performed to confirm the position of injection cannulae.

Behavioral Activity Quantification. Neck EMG or head acceleration signals were respectively high-pass filtered above 40 Hz and band-pass filtered between 2 and 20 Hz. The filtered signals were squared and smoothed with an averaged filter of 500 ms. The resulting signal provided a time-varying estimate of behavioral activity. Because the quality of EMG recording and the exact position of the accelerometer vary across days and between animals, the threshold value to separate immobility from mobility was adjusted manually. To this end, the time-varying behavioral estimate was overlaid with the simultaneously recorded ECoG. ECoG oscillatory content depends on behavioral activity, and this property was used to adjust precisely the threshold. The same threshold was used for control and drug recordings to be compared. If the interval between two consecutive mobility periods was less than 4 s, these periods were merged.

Power Spectrum Analysis. Spectral analyzes were made using a multitaper approach as implemented in the Chronux toolbox (http://chronux.org/). ECoG was digitally high-pass filtered at 1 Hz. Frequency-domain analysis was restricted to data recorded during immobility periods. Power spectrum density functions were computed with nine tapers and averaged over 10-s–long epochs.

High-Voltage Spindles Comparison. Comparison of high-voltage spindles (HVS) incidence and power between control and drug conditions was made from ECoG (25–30 min long) recorded during periods of immobility (i.e., periods of immobility, interleaved by behavioral activity, were concatenated until they amounted to 25–30 min). The rationale for comparing HVS over such relatively short periods was to avoid as much as possible the inclusion of slow-wave sleep in our control recordings. During immobility, the incidence of HVS in mice was extremely low in control condition but strongly and reliably increased after CP55940 systemic injection (6). Noticeably, across experiments and animals, we found variability in the mean frequency of the HVS appearing after CP55940 injections (range, 4–8 Hz). The first step of our HVS quantification consisted therefore in determining the cannabinoid-induced HVS frequency band. To avoid ECoG power at low frequencies (<3 Hz) contaminating the estimation of the HVS frequency band (owing to the presence 1/f pink noise in this type of signal), the ECoG obtained after CP55940 injection was detrended (locdetrend function in Chronux toolbox, 300-ms–long moving windows). The average power spectrum density function of the detrended ECoG was computed as described earlier. The HVS frequency band was defined as a 2-Hz–wide window centered around the peak of the power spectrum in the drug condition (Fig. S2*A*, *1*). Using a distinct method (7) to reduce 1/f pink noise in the ECoG resulted in similar results. Note that ECoG detrending was only done to define the HVS frequency band. CP55940 globally reduced the amplitude of the ECoG fluctuations (Fig. 1). To avoid this effect affecting HVS detection, the ECoGs to compare were standardized. Time–frequency spectrograms of the standardized ECoGs were computed (1-s–long windows, advanced in steps of 0.2 s; examples in Fig. 1*C* and Fig. S2*B*). For each window, the power in the HVS frequency band was calculated (Fig. S2 *A*, *2*). An arbitrary threshold for HVS detection was then defined as the mean plus 2 SDs of the HVS frequency band power values obtained in all of the windows (vehicle + CP55940, Fig. S2 *A*, *3*). HVS were defined as the times when four or more consecutive windows had power values in the HVS frequency band superior to the threshold (Fig. 1 *B* and *C* and Fig. S2 *A*, *4* and *B*). Finally, the time–frequency spectrograms of the ECoGs (nonstandardized) were computed as above. In the pharmacological conditions to compare (e.g., vehicle vs. CP55940), we computed the sum of the ECoG power in the HVS frequency band from the windows detected as part of an HVS (Fig. S2 *A*, *5*). These sums provide a quantification of HVS incidence and power during a single experiment. It is very important to note that the threshold is a relative value that depends on the intraexperiment variability of the ECoG power in the HVS frequency band. For instance, a strong increase in HVS after CP55940 injection would bias the threshold toward a high value. Consequently, the number of detected HVS after vehicle injection would be low. Conversely, if a CP55940 injection had little effect on HVS (as in the D1-CB1R$^{-/-}$ mice), the threshold would be low and more HVS would be detected in the control recording (this is the reason why baseline HVS incidence is higher in Fig. 3*C* than in Fig. 3*A*). Using this "relative" method to compare HVS in a given pharmacological condition (e.g., vehicle) between different animals or experiments is therefore meaningless. Only change in HVS power and incidence (calculated as the ratio "HVS in CP55940"/"HVS in vehicle") were compared across animals.

Statistics. To statistically assess electrophysiological differences between pharmacological conditions (e.g., vehicle vs. CP55940) in a given group of animals (e.g., WT mice) we used the Wilcoxon paired signed rank test (nonparametric test). To statistically assess differences in CP55940 effect between two groups of animals (e.g., WT vs. Glu-CB1R$^{-/-}$ mice) we used the Wilcoxon rank sum test (nonparametric test).

1. Monory K, et al. (2007) Genetic dissection of behavioural and autonomic effects of Delta(9)-tetrahydrocannabinol in mice. *PLoS Biol* 5(10):e269.
2. Monory K, et al. (2006) The endocannabinoid system controls key epileptogenic circuits in the hippocampus. *Neuron* 51(4):455–466.
3. Marsicano G, et al. (2003) CB1 cannabinoid receptors and on-demand defense against excitotoxicity. *Science* 302(5642):84–88.
4. Bellocchio L, et al. (2010) Bimodal control of stimulated food intake by the endocannabinoid system. *Nat Neurosci* 13(3):281–283.
5. Ledberg A, Robbe D (2011) Locomotion-related oscillatory body movements at 6-12 Hz modulate the hippocampal theta rhythm. *PLoS ONE* 6(11):e27575.
6. Ryan LJ (1984) Characterization of cortical spindles in DBA/2 and C57BL/6 inbred mice. *Brain Res Bull* 13(4):549–558.
7. Sirota A, et al. (2008) Entrainment of neocortical neurons and gamma oscillations by the hippocampal theta rhythm. *Neuron* 60(4):683–697.

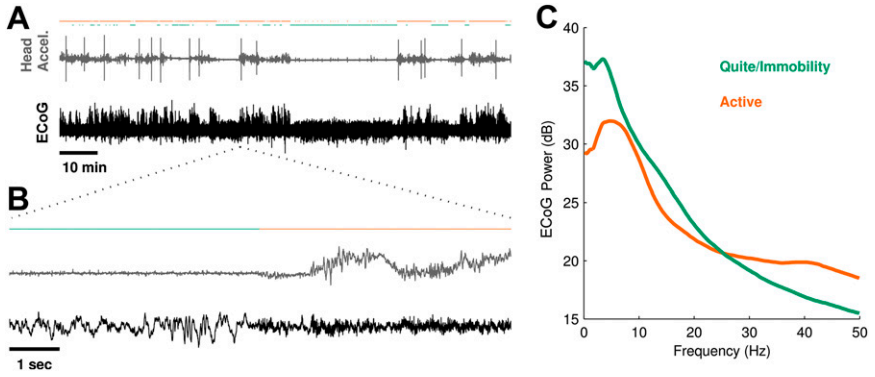

Fig. S1. Separation of immobility from mobility periods. (*A* and *B*) Illustrative experiment during which ECoG (black) and vertical head acceleration (gray) were recorded simultaneously. Orange and green lines show detected periods of activity and immobility, respectively. (*A*) Full recording; (B) 10-s epoch taken from *A*, at the time indicated by the dash lines. (*C*) Power spectrum density function of the ECoG during immobility and activity (same color code as in *A* and *B*). Note that the strong increase in ECoG power above 30 Hz during behavioral activity is partially accounted by contamination (via passive volume conduction) of the ECoG with electromyographic signals (mainly showing artifacts).

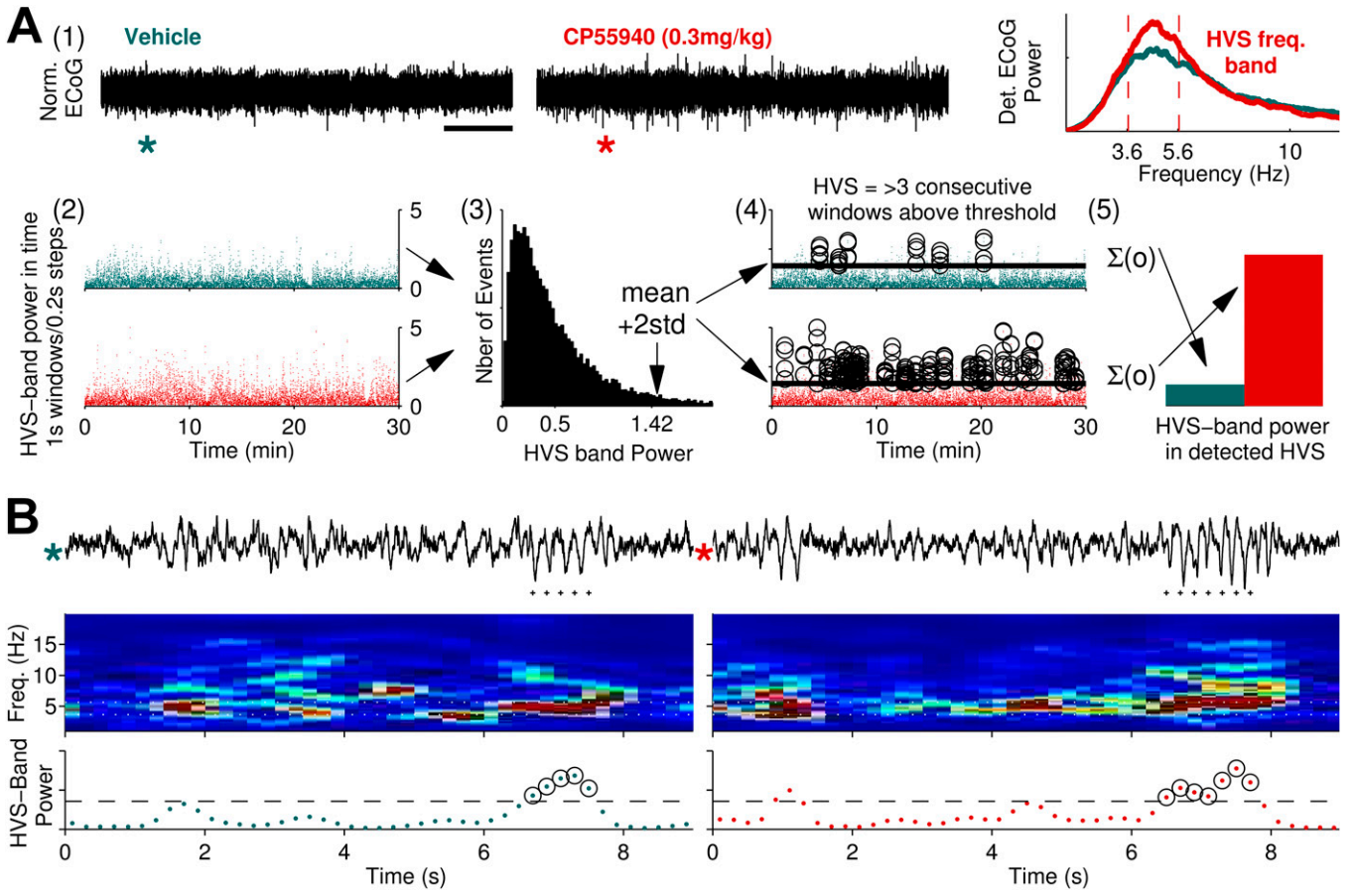

Fig. S2. Method to compare the incidence and power of HVS after vehicle and CP55940 injections. (*A*, *1*) Same-length ECoGs, recorded during immobility epochs, are compared after systemic injections of vehicle and CP55940. Power spectra of the detrended ECoGs are computed, and HVS frequency band is determined. (*A*, *2*) Time-frequency spectrograms are computed from the standardized ECoG, and the time-varying power in the HVS frequency band is reported. (*A*, *3*) Threshold detection is set as the mean plus 2 SDs of all the HVS band power values (vehicle + CP55940). (*A*, *4*) HVS are defined as at least four consecutive windows with power values above threshold. (*A*, *5*) The sum of the ECoG power (in the HVS band) from the windows detected as part of an HVS is computed for each pharmacological condition and compared. (*B*) Examples of detected HVS. (*Top*) Traces are ECoG epochs taken from *A*, at times indicated by stars. (*Middle*) Time–frequency spectrograms. White dotted lines show HVS frequency band for this experiment. (*Bottom*) ECoG power in the HVS frequency band. Dashed lines represent the threshold and circled points the values detected as part of a HVS.

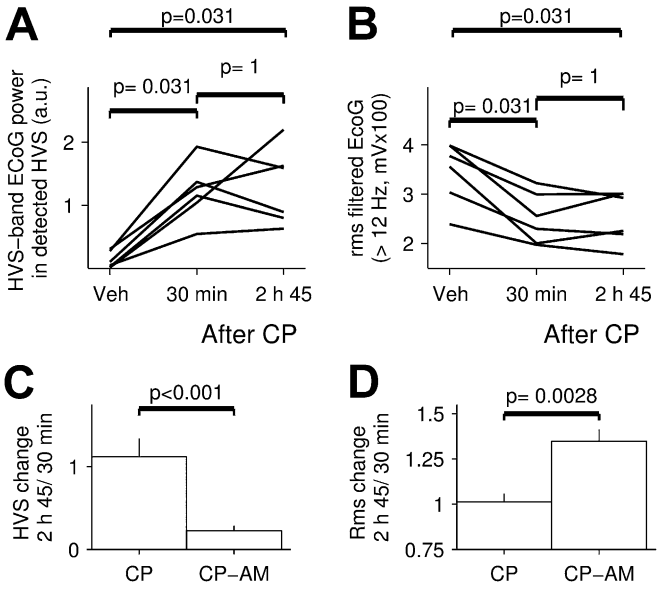

Fig. S3. CP55940 effects on HVS and fast ECoG oscillations are still present 2 h 45 min after injection and are reversed by injection of a CB1 antagonist. (*A*) HVS were compared in 30-min-long epochs (during immobility) starting 15 min after vehicle and both 15 min and 2 h 30 min after CP55940 injections (0.3 mg/kg, n = 6 experiments in six mice). (*B*) Same experiments as in *A*, but the amplitudes of fast ECoG oscillations (>12 Hz) were compared. *P* values in *A* and *B* are from Wilcoxon paired two-sided signed rank test. (*C*) Average ratio between late and immediate effects of CP55940 on HVS. Comparison is made between experiments in which only CP55940 was injected (left bar, same data as in *A*) and experiments in which an i.p. injection of AM251 was made 1 h after CP55940 injection (right bar, same data as in Fig. 1*D*). In both conditions late effects were quantified starting 2 h 30 min after the CP55940 injection. *P* value is from the Wilcoxon ranksum test. (*D*) Similar comparison as in *C*, but for the amplitude of fast (>12 Hz) ECoG oscillations. Left bar is calculated from from data in *B*, whereas right bar is from the same data as in Fig. 1*F*.

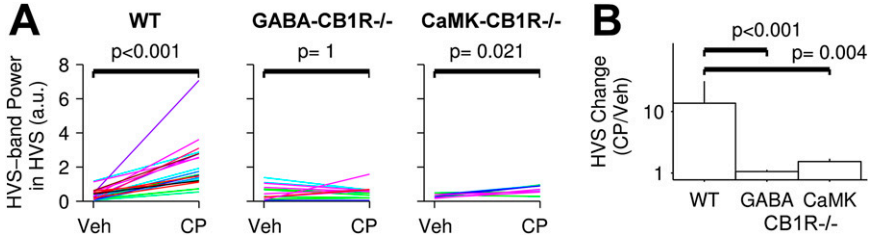

Fig. S4. Effect of CP55940 on HVS is abolished in mice lacking CB1R expression in forebrain GABAergic neurons (GABA-CB1R$^{-/-}$) and forebrain principal neurons (CaMK-CB1R$^{-/-}$). (*A*) HVS comparison in all experiments. Each line represents a single experiment, and different colors represent different animals. CP55940 (0.3 mg/kg) reliably increases HVS in WT animals. Such effect is absent in GABA-CB1R$^{-/-}$ mice and small in CaMK-CB1R$^{-/-}$ mice. *P* values are from Wilcoxon paired two-sided signed rank test. (*B*) Mean HVS change (CP55940/vehicle) + SEM for all experiments. *P* values are from Wilcoxon rank sum test vs. WT data. Note that in GABA-CB1R$^{-/-}$ and CaMK-CB1R$^{-/-}$ mice, CB1R expression is absent from D1-positive striatonigral neurons.

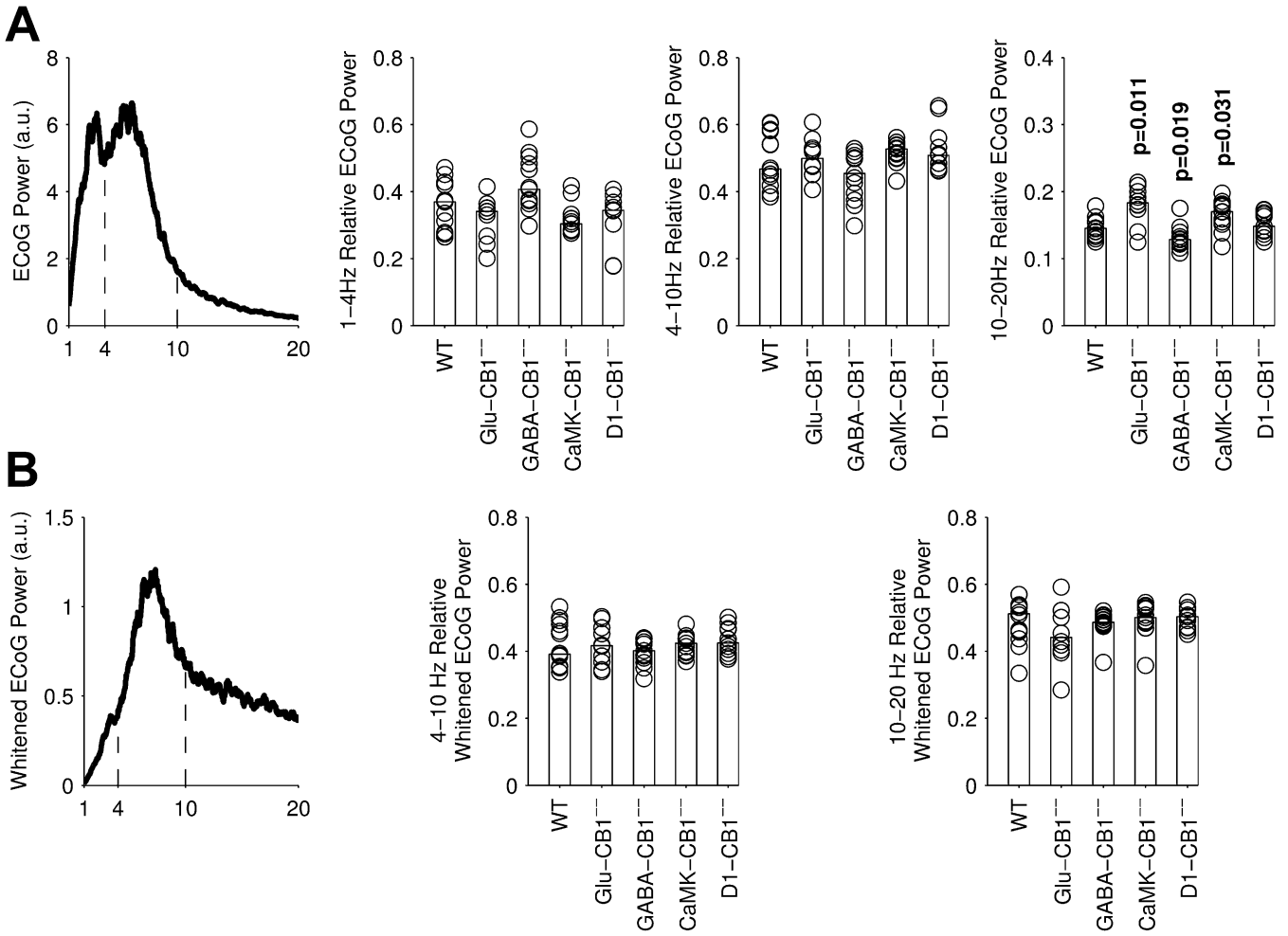

Fig. S5. Relative ECoG oscillatory content in control condition recorded from WT and CB1R conditional mutant mice. (*A*, *Left*) ECoG power spectrum density function of a representative WT mouse, in control condition. Three frequency bands (1–4, 4–10, 10–20 Hz) were arbitrarily defined. ECoG was high-pass filtered above 1 Hz. The three histograms show the ECoG relative power in the three bands during baseline or vehicle recordings for all experiments displayed in Figs. 2, 4, 5, and Fig. S4. *P* values are from Wilcoxon rank sum test vs. WT and were not graphically reported if above 0.05. (*B*) Same data as in *A*, except that the 1/f power relationship was removed from the ECoG (7). In this case, the relative power in the lowest frequency band is meaningless and is not shown. Note that there was no significant difference between WT and CB1 conditional mutant mice in the 10- to 20-Hz band.